Keto−Enol Isomerization of Acetaldehyde in HZSM5. A Theoretical Study Using the ONIOM2 Method

Xavier Solans-Monfort, Joan Bertran, Vicenç Branchadell, and Mariona Sodupe*

Departament de Química, Universitat Autònoma de Barcelona, Bellaterra 08193, Spain

Received: June 13, 2002; In Final Form: July 30, 2002

The keto−enol isomerization of acetaldehyde inside HZSM5 has been studied using the B3LYP density functional approach and different cluster models (T3, T5, and T63). For the largest cluster, which contains up to 63 tetrahedra, we have used the ONIOM2(B3LYP:MNDO) and ONIOM2(B3LYP:AM1) approaches. In all cases, calculations show that the zeolite produces an important catalytic effect on the enolization reaction and that the adsorption of acetaldehyde to the zeolite corresponds to a neutral H-bond complex. Enlarging the size of the cluster to T63 with ONIOM2 does not modify the nature of the interaction between the keto and enol forms of acetaldehyde with the zeolite. However, the embedding effects destabilize the keto intermediate and stabilizes the enol one, which results in a considerable decrease of the reaction energy. The ONIOM procedure allows us to naturally introduce the limited flexibility of the zeolite at a reasonable computational cost without imposing artificial constraints.

1. Introduction

Nowadays, zeolites are one of the most important industrial solid catalysts.[1] Although these catalysts are most commonly discussed in the context of chemical technologies such, as refining, there is increasing interest[2] in using zeolites for the synthesis of fine chemicals. Proton-exchanged zeolites present high acidity, and so, they are commonly used in acid-catalyzed reactions[3−5] such as double bond migration, skeletal reorganization, or aldol condensation.

The aldol condensation is a very important reaction in organic synthesis because it leads to the formation of C−C bonds. Because of that, the use of different catalysts and in particular the use of zeolites for the catalysis of this reaction has been considered by several authors.[3,6−13] The nature of adsorbed acetaldehyde and ketones on different zeolites has been studied by means of infrared spectroscopy,[8,9,14] NMR studies,[10,11,15] and theoretical calculations.[14−16] However, to our knowledge, the heat of adsorption of ketones on zeolites has only been measured for acetone.[15] On the other hand, the factors that control the catalytic activity and selectivity of the aldol condensation have also been discussed in experimental studies.[8−10,13] The proposed mechanism for the aldol condensation in zeolites assumes that the first step is the keto−enol isomerization of the aldehyde. In a second step the enol reacts with an aldehyde molecule that is coordinated to a Brønsted acid site of the zeolite.[8,9,13] Thus, the formation of the enol form of the aldehyde molecule, through a keto−enol isomerization, is a very important reaction in the aldol condensation. In fact, previous gas-phase studies have shown that this step is the crucial one.[17]

The keto−enol isomerization of acetaldehyde in the gas phase and catalyzed by solvent molecules has recently been studied in our group.[18] Results showed that in the gas phase the reaction is endothermic and presents a very high energy barrier (67.9 kcal/mol). Although solvent molecules produce an important catalytic effect, the energy barrier of the keto−enol isomerization is still high (40.6 kcal/mol). The catalytic effect of the solvent molecules is due to the formation of hydrogen bonds that contribute to stabilize the transition state and to a smaller geometry distortion of acetaldehyde along the process.

Zeolites present acidic and basic sites close enough to each other to exhibit bifunctional catalysis. On the other hand, because geometry distortions of acetaldehyde during the isomerization reaction are expected to be smaller in proton-exchanged zeolites than in the solvent-assisted process, the catalysis by zeolites might be more efficient.

To our knowledge, no theoretical study related to the keto−enol isomerization in proton-exchanged zeolites or any possible step of the aldol condensation in zeolites has been reported. The goal of the present study is to analyze the catalytic effect of HZSM5 on the keto−enol isomerization of acetaldehyde and compare it to that of water molecules.[18] A second goal of the present work is to discuss the behavior of different theoretical strategies within the ONIOM framework for studying this kind of systems. It must be pointed out that the ONIOM methodology has not yet been applied to study reactivity inside zeolites and only in a few cases for related materials.[19−21]

2. Computational Details

Two different strategies have been adopted to model the zeolite. The first one represents the active site of the zeolite by different clusters, and the second strategy uses the hybrid ONIOM methodology.[22] This approach subdivides the *real* system in different parts or layers, in our case two (ONIOM2), each one being described at a different level of theory. The most important one, which includes the active site of the zeolite, is called the *model* system and is described at the highest level of theory, whereas the rest of the zeolite is computed at a lower level. In this case the total energy of the system is obtained from three independent calculations:

$$E^{\mathrm{ONIOM2}} = E^{\mathrm{high}}_{\mathrm{model}} + E^{\mathrm{low}}_{\mathrm{real}} - E^{\mathrm{low}}_{\mathrm{model}} \quad (1)$$

This method can be viewed as an extrapolation scheme. Starting from $E^{\mathrm{high}}_{\mathrm{model}}$, the extrapolation to the real system $E^{\mathrm{low}}_{\mathrm{real}} - E^{\mathrm{low}}_{\mathrm{model}}$ is assumed to give an estimation for $E^{\mathrm{high}}_{\mathrm{real}}$.

10.1021/jp026303s CCC: $22.00
Published on Web 08/31/2002

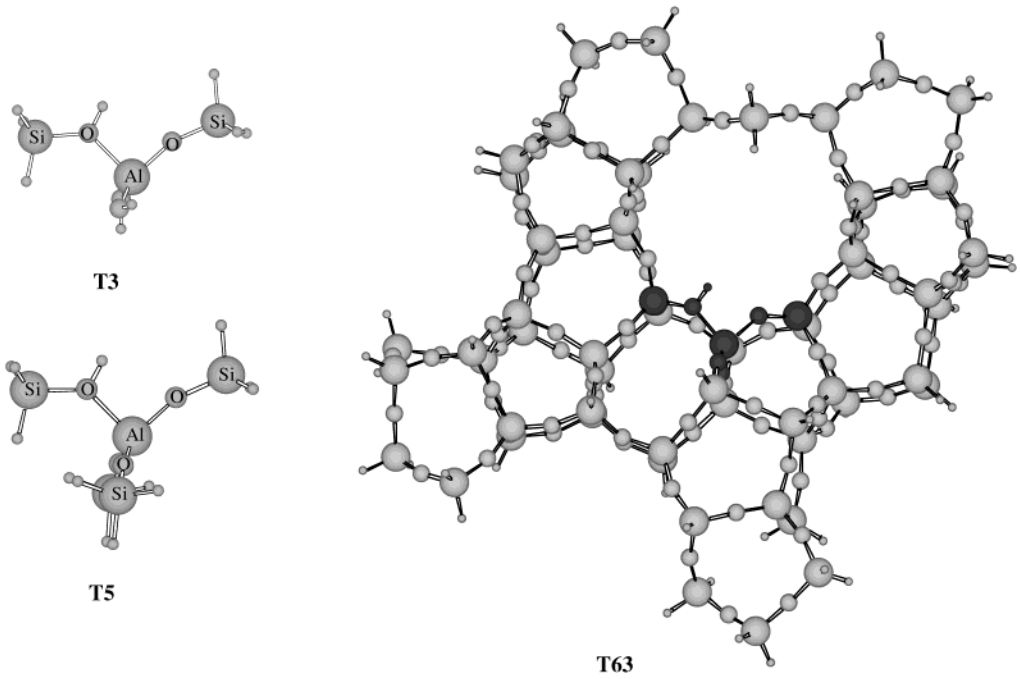

Figure 1. Clusters used to model the HZSM5 zeolite. The darker atoms in cluster T63 are treated at the higher level in the ONIOM2 approach.

2.1. Zeolite Models. Figure 1 presents the clusters used to model the zeolite. The simplest one (T3) consists of a tritetrahedral cluster [$H_3SiOAl(OH)_2OSiH_3$]. This cluster has been used in our group for studying the NO decomposition by Cu−ZSM5.[23−25] Other authors have also considered this model for studying the interaction of small molecules with Brønsted acidic sites of zeolites.[26−29] For this cluster we have introduced geometry constraints. The two silicon, aluminum, and oxygen atoms have been restricted to lie in the same plane, given that full optimizations lead to unreal interactions between the acetaldehyde and the terminal OH of the zeolite. Moreover, we have also performed calculations using a pentatetrahedral cluster [$(H_3SiO)_4Al$] (T5) to represent the active site of the zeolite. Such a cluster avoids the terminal OH groups, and so, no geometrical constraints have been imposed in this case.

ONIOM2 calculations have been performed over a T63 cluster. That is, the whole system contains 63 tetrahedra (218 atoms) and the strategy to build it was to include the 10-ring channel and to extend the system around the active site with a similar number of tetrahedra. We also avoided the SiH_3 terminations because the formation of five-member rings gives a more constrained geometry, closer to what is observed in the zeolite. The part considered at the highest level of theory, the model system, is equal to cluster T3 and has been represented with darker atoms in Figure 1.

2.2. Level of Theory. Geometry optimizations and harmonic vibrational frequencies have been computed using the nonlocal hybrid three-parameter B3LYP[30] density functional approach and the 6-31++G(d,p) basis set. It should be mentioned that density functional methods do not take into account the dispersion energy. However, the systems studied in the present work interact with the acid site of the zeolite through medium-strong H-bonds, and so, dispersion forces are only a minor component of the hydrogen bond interaction. Because of that, the computed B3LYP interaction energies are expected to be reasonably accurate. In fact, previous calculations on the interaction of small molecules with the isolated hydroxyl of silica and Brønsted acid sites in zeolites have shown that the B3LYP interaction energies are similar to the ones obtained with MP2,[31] the most economical post-Hartree−Fock method that accounts for the full range of intermolecular interactions: electrostatics, induction, and dispersion.

To test the effect of further enlarging the basis set, we have also performed single point B3LYP calculations with the 6-311++G(2d,2p) basis set for the stationary points obtained with the T3 cluster. The results obtained show that the effect of enlarging the basis set is small at this level of calculation, the largest variation being about 1.3 kcal/mol. Because of that, and for comparison purposes, we will only report the results with the 6-31++G(d,p) basis set, given that the calculations of the T5 cluster and those of the model system in the ONIOM2 approach have only been performed with the smaller basis set.

Basis set superposition error has been corrected using the counterpoise procedure.[32] The computed counterpoise correction ranges from 1 to 2 kcal/mol, which represents about 10−15% of the H-bond interaction energy. For the transition state, the counterpoise correction has been computed by assuming the same two fragments considered for the HZ(enol) intermediate. We have chosen this partition because the geometry of the transition state is product-like. Thermodynamic corrections have been obtained at 298.15 K and 1 atm assuming an ideal gas, unscaled harmonic vibrational frequencies, and the rigid rotor approximation by standard statistical methods.[33]

The model system in the ONIOM2 calculations is the T3 cluster and is described using the B3LYP functional and the 6-31++G(d,p) basis set. For the low-level part we have tested two different semiempirical methods: MNDO[34] and AM1.[35] These two methods have been used previously[19] in ONIOM calculations to model the NH_3 adsorption at the isolated hydroxyl group of the silica surface. Roggero et al.[19] conclude that although the B3LYP:MNDO combination gives better silica geometries and vibrational frequencies than the B3LYP:AM1 one, the latter provides a better description of hydrogen bonds, the interaction energies being closer to those obtained with higher levels of theory. All calculations have been performed using the GAUSSIAN98 package.[36]

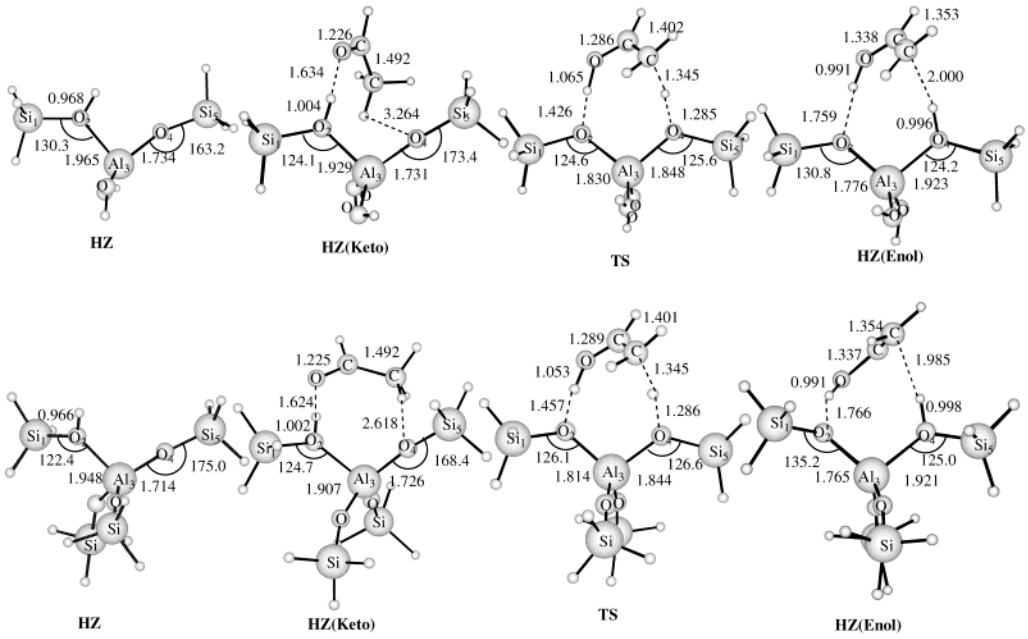

Figure 2. B3LYP-optimized geometries of the stationary points of the keto−enol isomerization reaction obtained with clusters T3 and T5. Distances are in Å, and angles, in degrees.

3. Results and Discussion

3.1. Cluster Results. Figure 2 shows the optimized structures of the stationary points (reactant, transition state, and product) corresponding to the keto−enol isomerization reaction, located with clusters T3 and T5. Because both clusters provide quite similar results and T3 is the model system used in the ONIOM2 calculations, we will mainly refer to the results obtained with this cluster during the discussion. Finally, we will briefly point out the observed differences.

It can be observed that acetaldehyde interacts with the zeolite through a hydrogen bond between the carbonylic oxygen and the acid O_2H group of the zeolite. This hydrogen bond is nearly linear and presents a short O_2H-O distance (1.634 Å). Consequently, the zeolitic O_2-H distance increases considerably (from 0.968 to 1.004 Å) and the O_2H stretching frequency is strongly downshifted (-719 cm^{-1}). This shift of the Brønsted acid site, although smaller than the one that would be expected considering the proton affinity of acetaldehyde,[37] corresponds to a medium-strong hydrogen bond. The counterpoise-corrected binding energy (11.9 kcal/mol) is consistent with the energetical classification[38] for a medium-strong H-bond, because the stabilization due to the $CH-O_4$ interaction is expected to be small. This H-bond interaction is similar to that previously determined at the MP2 level and correcting for basis set superposition error (13.9 kcal/mol).[16] Calculations for acetone provide similar H-bond interactions.[14−16] However, the experimentally determined heat of adsorption of acetone[15] on HZSM5 (31.1 kcal/mol) is much larger than the theoretical values. This difference has been attributed to "nonlocal interactions"; that is, to the confinement effect due to the structure of the zeolite cavity and the interactions of polarizable framework atoms with acetone, and to the long-range electrostatic forces, which have been approximated by the heat of adsorption of acetone in silicalite (16.0 kcal/mol).[15] However, as will be shown in the ONIOM subsection, enlarging the zeolite cluster to 63 tetrahedra, which supposedly should include part of these "nonlocal" interactions, does not increase the adsorption energy of acetaldehyde. Therefore, the difference must be attributed to other kinds of binding forces.

On the other hand, the hydrogen bond interaction between acetaldehyde and the acid site of the zeolite produces a red shift of the C═O stretching mode. Experimental studies[9] on adsorbed acetaldehyde on HZSM5 provide a band at 1703 cm^{-1}, which is assigned to this C═O stretching vibration. This value is smaller than the one computed at the B3LYP level (1771 cm^{-1}). However, if one scales the computed frequencies by 0.9614 to account for both systematic errors on the calculation of the force constant and the lack of anharmonic effects,[39] one obtains a value of 1700 cm^{-1}, in very good agreement with the experimental observations. Moreover, the computed shift (scaled) of 42 cm^{-1} is in very good agreement with the experimental one of 40 cm^{-1}.[9]

Our results are in contrast to what has been suggested in the experimental study of Chavez et al.,[9] which states that the primary interaction between acetaldehyde and the zeolite surface corresponds to a proton-transferred structure, that is, to an ion pair. It should be pointed out that all our attempts to optimize such a structure have spontaneously evolved to the keto form of acetaldehyde. Considering the good agreement between the computed and experimental CO frequency and shifts, the observed species in the adsorption of acetaldehyde on HZSM5 does not seem to be protonated acetaldehyde but neutral acetaldehyde. On the other hand, the shift of CO would be much larger if acetaldehyde were protonated. Gas-phase calculations indicate that the frequency of CO decreases about 150 cm^{-1} upon protonation. The present results are in agreement with the experimental studies of Paukshtis et al.,[40] who concluded that the formation of the ion pair is only favorable if the difference in proton affinities between the substrate and the zeolite is less than 85 kcal/mol. For the present system such a difference is computed to be 118 kcal/mol. Furthermore, ^{13}C NMR studies of acetaldehyde adsorbed on HZSM5 indicate that at low coverages acetaldehyde is bound to the acid site through a hydrogen bond interaction.[11]

The enol form of acetaldehyde, hydroxyethylene, interacts with the zeolite through two hydrogen bonds: one in which the enol acts as proton donor and another in which it acts as proton acceptor. The first one occurs between the hydroxyl

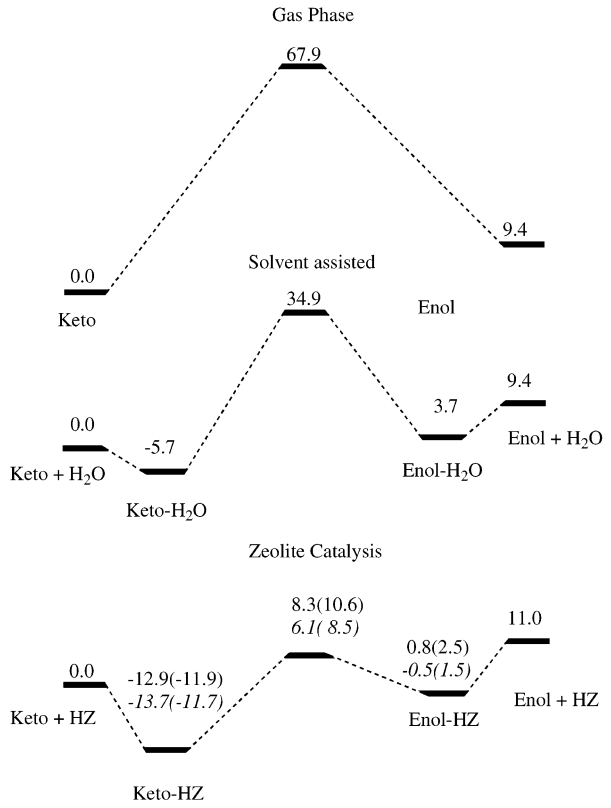

Figure 3. Potential energy diagram of the keto−enol isomerization of acetaldehyde in the gas phase, catalyzed by a water molecule and inside HZSM5. Relative energies with respect to the keto + catalyst asymptote (kcal/mol). Plain numbers correspond to T3 results, and italic numbers, to T5. In parentheses are counterpoise-corrected values.

group and the O_2 atom of the zeolite, and the second one, between the acid site O_4H of the zeolite and the π system of the enol. The frequency shift of the Brønsted acid site is −594 cm^{-1}, smaller than for the keto form. This is not surprising considering the larger hydrogen bond distances and the weaker interaction. Note that the counterpoise-corrected binding energy (8.5 kcal/mol) is smaller than that obtained for the HZ(keto) intermediate even though it accounts for two hydrogen bond interactions.

The structure of the transition state is also shown in Figure 2. It can be observed that its geometry is closer to the product than to the reactant, as should be expected for an endothermic reaction (see below). The alcohol is nearly formed whereas the other proton lies halfway between the C and O_4. Moreover, the zeolite presents some reorganization. The main changes correspond to the Al_3-O_2 and Al_3-O_4 distances, those related to the catalytic process, and to the $Al_3O_4Si_5$ angle. The Al_3-O_2 distance decreases 0.099 Å, whereas the Al_3-O_4 distance increases around 0.117 Å. Consequently, in the transition state both distances are similar. The $Al_3O_4Si_5$ angle decreases 47.8°. It should be noted that this important change on the $Al_3O_4Si_5$ angle is due to the fact that the mechanical embedding is not considered in these cluster calculations.

Figure 3 shows the energetics of the keto−enol isomerization in the gas phase, catalyzed by a water molecule and inside the zeolite using clusters T3 and T5. The gas-phase and water-catalyzed results have been taken from ref 18. It should be noted that the basis set used in that study was not the same as the one used in the present work. This explains the different asymptotic behaviors, that is, the relative energy of the keto and enol forms of acetaldehyde. It can be observed that for the water-assisted system, both intermediates show the same interaction energy

TABLE 1: Relative Energies (kcal/mol) with Respect to the HZ + Keto Asymptote Obtained with the T3 Cluster[a]

	HZ + keto	HZ(keto)	TS	HZ(enol)	HZ + enol
ΔE	0.0	−12.9(−11.9)	8.3(10.6)	0.8(2.5)	11.0
ΔH°_{298}	0.0	−11.4(−10.4)	6.6(8.9)	2.7(4.4)	11.5
ΔG°_{298}	0.0	0.1(1.1)	19.4(21.7)	15.5(17.2)	12.3

[a] In parentheses are counterpoise-corrected values.

(5.7 kcal/mol), and thus, the reaction energy from hydrated-keto to hydrated-enol is the same (9.4 kcal/mol) as the one obtained for the isolated system. For the zeolite-catalyzed system it is observed that the interaction energies of the enol and keto forms of acetaldehyde with the zeolite are significantly much larger. This could be easily understood if one considers that the zeolite is more acidic than water and its shape is more appropriate to stabilize the H-bonded intermediates. Because the zeolite interacts stronger with acetaldehyde than with hydroxyethylene, the reaction energy of the keto−enol process becomes slightly less favorable inside the zeolite (13.7 kcal/mol) than in the gas phase (11.0 kcal/mol). This value increases slightly (14.4 kcal/mol) when correcting for BSSE.

The transition state for the isomerization reaction lies 8.3 kcal/mol above the HZ + keto asymptote, the energy barrier being 21.2 kcal/mol from the HZ(keto) intermediate. As can be observed, the catalytic effect of the zeolite is much more important than that of water. The transition state of the reaction is largely stabilized with respect to the ground-state asymptote. Moreover, the energy barrier computed with respect to the keto intermediate is much lower for the zeolite-catalyzed system (21.2 kcal/mol) than for the water-assisted (40.6 kcal/mol) or the gas-phase (67.9 kcal/mol) systems. This stronger catalytic effect is due to a smaller geometry reorganization of the system along the process and also to the high acidity of the zeolite, which facilitates the proton transfer to acetaldehyde.

The real catalytic effect can be observed from the comparison between the activation free energy in the gas phase and inside the zeolite. The thermodynamic functions at 298.15 K are given in Table 1. Counterpoise-corrected values are included in parentheses. The $\Delta G^{\ddagger}_{298}$ for the keto−enol isomerization inside the zeolite is 19.4(21.7) kcal/mol with respect to the HZ + keto asymptote and 19.3(20.6) kcal/mol with respect to the HZ(keto) intermediate. As expected, entropic effects destabilize the transition state with respect to the HZ + keto asymptote but modify only slightly the energy barrier with respect to the HZ-(keto) intermediate. The $\Delta G^{\ddagger}_{298}$ value of 19.4 kcal/mol is much smaller than that corresponding to the uncatalyzed (64.9 kcal/mol) or the water-assisted (44.3 kcal/mol) systems. This great catalytic activity is in good agreement with the experimental results which report an easy and fast conversion of acetaldehyde to the aldol adduct.[9,11]

Finally, let us compare the results obtained with clusters T3 and T5. It can be observed in Figure 2 that the geometry parameters related to the zeolite−acetaldehyde interaction are very similar in all the stationary points. The main difference appears in the HZ(keto) intermediate, which shows a different interaction between the methyl group of acetaldehyde and the oxygens bonded to aluminum. This is due to the fact that in cluster T3 these oxygens are of different nature (−OH and $-OSiH_3$), the presence of terminal −OH inducing the changes in the acetaldehyde orientation. On the other hand, the results obtained with cluster T5 show that the dihedral angles defined by the Si_1, O_2, Al_3, O_4, and Si_5 atoms are far from 180°, the value imposed in the T3 cluster calculations to avoid unreal hydrogen bond interactions. The computed values of these

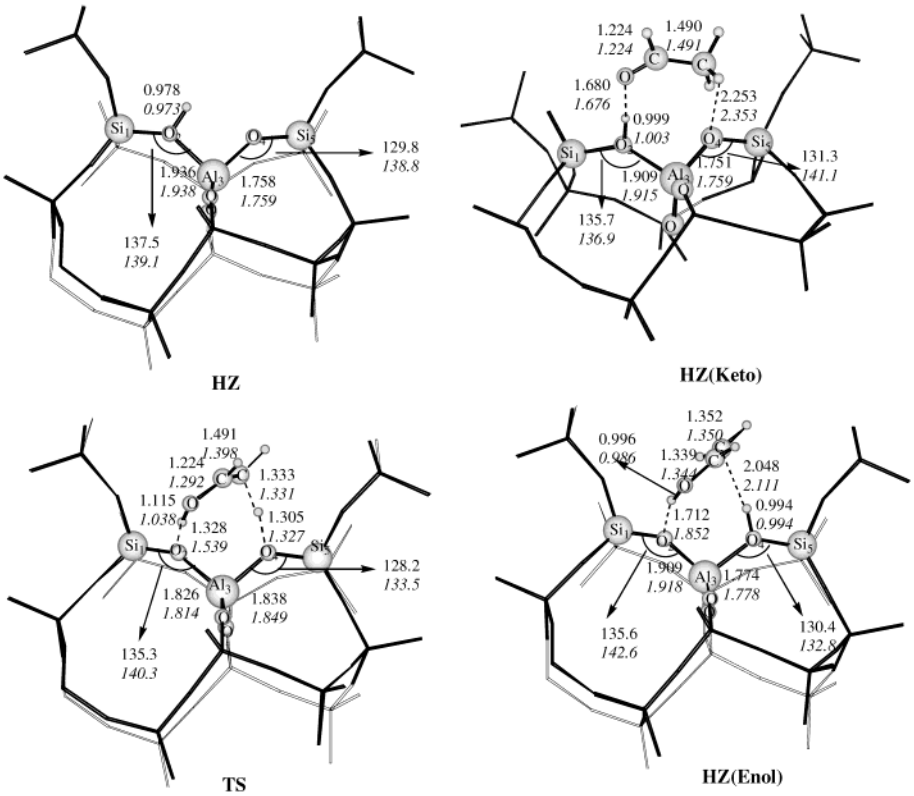

Figure 4. Main geometrical parameters of the stationary points of the keto−enol isomerization reaction obtained with cluster T63 with the ONIOM2-(B3LYP:MNDO) and *ONIOM2(B3LYP:AM1)* approaches. Distances are in Å, and angles, in degrees.

dihedral angles, which range from 120° to 160° can, however, be the result of a lack of mechanical constraints in the zeolite. This aspect will be considered and discussed in the next section in which ONIOM2 calculations for a T63 cluster will be presented. The energy profiles obtained with both T3 and T5 are very similar (see Figure 3). The most remarkable is that the HZ(enol) and the TS structures are slightly more stable with the larger cluster.

3.2. ONIOM Calculations. Figure 4 presents the ONIOM2-optimized geometries corresponding to the stationary points of the keto−enol isomerization inside HZSM5. For simplicity we have only included the geometrical parameters of the active site or model system.

The comparison between the ONIOM2 results (Figure 4) and the ones obtained with the T3 and T5 clusters (Figure 2) shows that there are not dramatic changes in the zeolite−acetaldehyde interaction when the cluster is increased to 63 tetrahedra with the ONIOM2 procedure. Nevertheless, there are some differences on the structure of the zeolite that are worth mentioning. On one hand, it can be observed that the T3 and T5 calculations provide values of the $Al_3O_4Si_5$ angle in HZ and in the HZ-(keto) intermediate that are too large. This is due to the fact that T3 and T5 clusters are too small to take into account the constraints induced by the zeolite framework. The $Al_3O_4Si_5$ angle is not so large in the transition state or the enol-adsorbed intermediate because the O_4 atom is protonated or almost protonated. On the other hand, ONIOM2 calculations show that the dihedral angles defined by the Si_1, O_2, Al_3, O_4, and Si_5 atoms do not change very much along the HZ(keto) → HZ(enol) process, the largest variation being about 5−6°. However, for the T5 cluster calculations the variations of the dihedral angles are much larger. This is again due to the larger flexibility of the T5 cluster compared to the T63 one considered in the ONIOM calculations.

Let us now analyze the differences between the results obtained with the two B3LYP:MNDO and B3LYP:AM1 method combinations used in the ONIOM2 procedure. In general, the optimized geometries are quite similar in both methods. The most significant difference appears in the transition state for the O_2−HO− distance. At the B3LYP:AM1 level the proton of the zeolite is completely transferred to acetaldehyde, whereas this is not the case with B3LYP:MNDO. This is probably related to the fact that the computed deprotonation energy of the zeolite at the B3LYP:AM1 level (304.5 kcal/mol) is smaller than that at the B3LYP:MNDO level (327.0 kcal/mol). Considering that AM1 provides a better description of the hydrogen-bonded systems, and that the B3LYP:AM1 deprotonation energy is in much better agreement with previous QM-pot calculations[41] than the B3LYP:MNDO one, we expect the B3LYP:AM1 results to be more reliable. Moreover, a previous ONIOM study[19] on the interaction of NH_3 with the hydroxyl group of the silica surface has shown that among the three semiempirical methods AM1, MNDO, and PM3 used for the real system, AM1 provides better results.

Table 2 presents the energetics of the process. For comparison we have also included the values obtained with clusters T3 and T5. It can be observed that ONIOM2 calculations provide a smaller interaction energy between acetaldehyde and the zeolite. This destabilization of the HZ(keto) intermediate is more important with B3LYP:MNDO than with B3LYP:AM1. In contrast, the HZ(enol) intermediate becomes slightly more stable in the ONIOM calculations. As a result, the reaction energy of the HZ(keto) → HZ(enol) process becomes smaller. The reaction energy of 13.7 kcal/mol with T3(B3LYP) decreases to 5.9 kcal/mol with T63(B3LYP:MNDO) and to 7.4 kcal/mol with T63-(B3LYP:AM1). On the other hand, given that the energy of the transition state with respect to the HZ + keto asymptote is very similar with both the T3 and T63 clusters, the energy barrier

TABLE 2: Relative Energies (kcal/mol) with Respect to the HZ + Keto Asymptote Obtained with T3, T5, and T63 Clusters[a]

	HZ + keto	HZ(keto)	TS	HZ(enol)	HZ + enol
T3(B3LYP)	0.0	−12.9	+8.3	0.8	11.0
T5(B3LYP)	0.0	−13.7	+6.1	−0.5	11.0
T63(B3LYP:MNDO)	0.0	−7.4	+8.6	−1.5	11.0
high level	0.0	−11.9	+5.4	−2.1	
low level	0.0	+4.5	+3.2	+0.6	
T63(B3LYP:AM1)	0.0	−9.3	+8.7	−1.9	11.0
high level	0.0	−11.2	+6.0	−1.0	
low level	0.0	+1.9	+2.7	−0.9	

[a] Relative energies corresponding to ONIOM2 calculations for cluster T63 have been decomposed in two components: the high level, ΔE^{high}_{model}, and the low level, $\Delta(E^{low}_{real} - E^{low}_{model})$.

of the HZ(keto) → HZ(enol) isomerization energy decreases somewhat when the size of the cluster is increased. Despite that, if one considers entropic effects similar to the ones computed for T3 (see Table 1), the catalytic behavior will remain more or less the same in all cases.

The embedding effects introduced with ONIOM can be analyzed by decomposing the global interaction energy in two terms: the high-level (HL) contribution of the model system and the low-level (LL) contribution which account for the effects of increasing the size of the cluster. The HL term corresponds to the B3LYP energies of the model system but at the ONIOM-optimized geometries. Comparing the HL term of the two approaches, one could notice that the relative energies of the high-level part are similar in both cases. Thus, we conclude that ONIOM B3LYP:MNDO and B3LYP:AM1 produce similar constraints on the active site, which leads to very similar geometries and relative energies.

The HL values are also similar to the relative energies obtained with cluster T3. This is due to the fact that the geometry and energy changes of the model system induced by the larger rigidity of the T63 cluster are quite constant along the process. Despite this, there are small differences that are worth mentioning. If one compares the absolute B3LYP energy obtained with the T3 system with that of the model system in the ONIOM2 calculation, it is observed that the geometrical changes of the active site introduced by the T63 cluster are destabilizing, even though the constraints of the dihedral angles are released in the larger cluster. It is interesting to mention that, although this destabilization arises from many changes on distances and angles, part of it comes from the changes produced on the SiOAl angles and on the SiOAlO dihedral angles. As mentioned previously, the $Al_3O_4Si_5$ angle was computed to be too large in the initial asymptote and in the HZ(keto) intermediate with T3. Because of that and all the geometry changes induced by the T63 cluster, the model system in the asymptote (HZ) and in the first HZ(keto) intermediate is destabilized 2−3 kcal/mol more than in the TS or in the second HZ(enol) intermediate. As a result, the B3LYP relative energy of the transition state and HZ(enol) are somewhat smaller in the ONIOM2 calculations than in the T3 ones. It is interesting to notice that these results are similar to those obtained with cluster T5.

The second term, the low-level one, corresponds to the energy difference between the real and the model system at the low level of calculation (AM1 or MNDO). It includes (at the low level of calculation) two important factors, a destabilizing one arising from the distortion of the zeolite upon adsorption of acetaldehyde and a stabilizing one produced by the polarization of the model system by the rest of the zeolite. It can be observed in Table 2 that this low-level contribution is destabilizing in all cases except for the HZ(enol) intermediate at the AM1 level. Although the B3LYP:AM1 low-level destabilizing contribution is smaller than that for the B3LYP:MNDO one, both approaches follow the same trend along the reaction: the LL term is smaller in the product than in the reactant. This can be due to the fact that polarization of the model system by the zeolite is larger for the enol form (more polarizable) than for the keto one. Because long-range forces of electrostatic nature are expected to increase polarization effects, periodic calculations might decrease somewhat more the reaction energy.

Overall, we can say that T3 and T5 clusters provide a quite reasonable picture of the structure and energetics of the species involved in the keto−enol isomerization of acetaldehyde. However, enlarging the cluster with the ONIOM procedure allows us to introduce the characteristic building blocks of the zeolite, as well as to constrain the geometry optimizations of the active site by introducing the zeolite framework.

4. Conclusions

The keto−enol isomerization of acetaldehyde inside HZSM5 has been studied using the B3LYP density functional approach and modeling the zeolite with T3 and T5 clusters. Moreover, the effect of enlarging the cluster to T63 has been considered using the ONIOM2 approach and combining the B3LYP method with the AM1 or MNDO semiempirical ones. It is observed that the zeolite produces an important catalytic effect on the enolization reaction. The catalytic effect is much larger than that produced by a water molecule, due to the larger acidity of the zeolite and to smaller geometry reorganizations along the process. Calculations with all clusters indicate that the adsorption of acetaldehyde to the zeolite corresponds to a neutral complex and not to an ion pair.

Results with clusters T3 and T5 are very similar. Enlarging the size of the cluster to 63 tetrahedra with the ONIOM2 approach destabilizes the keto intermediate and stabilizes the enol one, which results in a decrease of the endothermicity of the reaction. The computed energy barrier and reaction energy of the HZ(keto) → HZ(enol) reaction at the ONIOM2(B3LYP:AM1) level are 18.0 and 7.4 kcal/mol, respectively. The ONIOM2 procedure allows us to consider quite large clusters at a reasonable computational cost, which naturally introduce the limited flexibility of the zeolite without imposing artificial constraints.

Acknowledgment. Financial support from DGICYT, through the PB98-0912 project, and the use of the computational facilities of the Catalonia Supercomputer Center are gratefully acknowledged. M.S. is indebted to DURSI of the Generalitat de Catalunya for financial support. X.S.M. acknowledges the Generalitat de Catalunya for a doctoral fellowship. P. Ugliengo and F. Maseras are acknowledged for helpful discussion.

References and Notes

(1) *Advanced zeolite Science and Applications*; Jansen, J. C., Stöcker, M., Karge, H. G., Weitkamp, J., Eds.; Elsevier: Amsterdam, 1994.
(2) Sen, S. E.; Smith, S. M.; Sullivan, K. A. *Tetrahedron* **1999**, *55*, 12657 and references therein.
(3) Hölderich, W.; Hesse, M.; Näumann, F. *Angew. Chem., Int. Ed. Engl.* **1988**, *27*, 226.
(4) Corma, A. *Chem. Rev.* **1995**, *95*, 559.
(5) van Santen, R. A.; Kramer, G. J. *Chem. Rev.* **1995**, *95*, 637.
(6) Hägen, G. P. US Pat. 4,433,174 (Standard Oil Co. (Indiana)), February 21, 1984.
(7) Höelderich, W.; Hupfer, L.; Schneider, K. US Pat 4,866,210 (BASF Aktiengesellschaft (Ludwigshafen)), September 12, 1989.
(8) Kubelková, L.; Novákova, J. *Zeolites* **1991**, *11*, 822.
(9) Chavez Diaz, C. D.; Locatelli, S.; Gonzo, E. E. *Zeolites* **1992**, *12*, 851.

(10) Xu, T.; Munson, E. J.; Haw, J. F. *J. Am. Chem. Soc.* **1994**, *116*, 1962.

(11) Biaglow, A. I.; Šepa, J.; Gorte, R. J.; White, D. *J. Catal.* **1995**, *151*, 373.

(12) Gorte, R. J.; White, D. *Top. Catal.* **1997**, *4*, 57.

(13) Dumitriu, E.; Hulea, V.; Fechete, I.; Auroux, A.; Lacaze, J.-F.; Guimon, C. *Micropor. Mesopor. Mater.* **2001**, *43*, 341.

(14) Florian, J.; Kubelková, L. *J. Phys. Chem.* **1994**, *98*, 8734.

(15) Šepa, J.; Lee, C.; Gorte, R. J.; White, D.; Kassab, E.; Evleth, E. M.; Jessri, H.; Allavena, M. *J. Phys. Chem.* **1996**, *100*, 18515.

(16) Kassab, E.; Jessri, H.; Allavena, M.; White, D. *J. Phys. Chem. A* **1999**, *103*, 2766.

(17) Coitiño, E. L.; Tomasi J.; Ventura, O. N. *J. Chem. Soc., Faraday Trans.* **1994**, *90*, 1745.

(18) Rodríguez-Santiago, L.; Vendrell, O.; Tejero, I.; Sodupe, M.; Bertran, J. *Chem. Phys. Lett.* **2001**, *334*, 112.

(19) Roggero, I.; Civalleri, B.; Ugliengo, P. *Chem. Phys. Lett.* **2001**, *341*, 625.

(20) Damin, A.; Bordiga, S.; Zecchina, A.; Lamberti, C. *J. Chem. Phys.* **2002**, *117*, 226.

(21) (a) Lopez, N.; Pacchioni, G.; Maseras, F.; Illas, F. *Chem. Phys. Lett.* **1998**, *294*, 611. (b) Ricci, D.; Pacchioni, G.; Szymanski, M. A.; Shluger, A. L.; Stoneham, A.; Marshall *Phys. Rev. B* **2001**, *64*, 224104.

(22) (a) Maseras, F.; Morokuma, K. *J. Comput. Chem.* **1995**, *16*, 1170. (b) Vreven, T.; Morokuma, K. *J. Comput. Chem.* **2000**, *21*, 1419.

(23) Rodríguez- Santiago, L.; Sierka, M.; Branchadell, V.; Sodupe, M.; Sauer, J. *J. Am. Chem. Soc.* **1998**, *120*, 1545.

(24) Solans-Monfort, X.; Branchadell, V.; Sodupe, M. *J. Phys. Chem. A* **2000**, *104*, 3225.

(25) Solans-Monfort, X.; Branchadell, V.; Sodupe, M. *J. Phys. Chem. B* **2002**, *106*, 1372.

(26) Jobic, H.; Tuel, A.; Krossner, M.; Sauer, J. *J. Phys. Chem.* **1996**, *100*, 19545.

(27) Krossner, M.; Sauer, J. *J. Phys. Chem.* **1996**, *100*, 6199.

(28) Kotrla, J.; Nachtigallová, D.; Bosáček, V.; Nováková, J. *Phys. Chem. Chem. Phys.* **1999**, *1*, 2613.

(29) Vos, A. M.; De Proft, F.; Schoonheydt, R. A.; Geerlings, P. *Chem. Commun.* **2001**, 1108.

(30) (a) Becke, A. D. *J. Chem. Phys.* **1993**, *98*, 5648. (b) Lee, C.; Yang, W.; Parr, R. G. *Phys. Rev. B* **1988**, *37*, 785. (c) Stephens, P. J.; Devlin, F. J.; Chabalowski, C. F.; Frisch, M. J. *J. Phys. Chem.* **1994**, *98*, 11623.

(31) Civalleri, B.; Garrone, E.; Ugliengo, P. *J. Phys. Chem. B* **1998**, *102*, 2373.

(32) Boys, S. F.; Bernardi, F. *Mol. Phys.* **1970**, *19*, 553.

(33) McQuarrie, D. *Statistical Mechanics*; Harper and Row: New York, 1986.

(34) Dewar, M. J. S.; Thiel, W. *J. Am. Chem. Soc.* **1977**, *99*, 4907.

(35) Dewar, M. J. S.; Zoebisch, E. G.; Healy, E. F.; Stewart, J. J. P. *J. Am. Chem. Soc.* **1985**, *107*, 3902.

(36) Frisch, M. J.; Trucks, G. W.; Schlegel, H. B.; Scuseria, G. E.; Robb, M. A.; Cheeseman, J. R.; Zakrzewski, V. G.; Montgomery, J. A., Jr.; Stratmann, R. E.; Burant, J. C.; Dapprich, S.; Millam, J. M.; Daniels, A. D.; Kudin, K. N.; Strain, M. C.; Farkas, O.; Tomasi, J.; Barone, V.; Cossi, M.; Cammi, R.; Mennucci, B.; Pomelli, C.; Adamo, C.; Clifford, S.; Ochterski, J.; Petersson, G. A.; Ayala, P. Y.; Cui, Q.; Morokuma, K.; Malick, D. K.; Rabuck, A. D.; Raghavachari, K.; Foresman, J. B.; Cioslowski, J.; Ortiz, J. V.; Baboul, A. G.; Stefanov, B. B.; Liu, G.; Liashenko, A.; Piskorz, P.; Komaromi, I.; Gomperts, R.; Martin, R. L.; Fox, D. J.; Keith, T.; Al-Laham, M. A.; Peng, C. Y.; Nanayakkara, A.; Gonzalez, C.; Challacombe, M.; Gill, P. M. W.; Johnson, B.; Chen, W.; Wong, M. W.; Andres, J. L.; Gonzalez, C.; Head-Gordon, M.; Replogle, E. S.; Pople, J. A. *Gaussian 98*, revision A.7; Gaussian, Inc.: Pittsburgh, PA, 1998.

(37) Pazé, C.; Bordiga, S.; Lamberti, C.; Salvalaggio, M.; Zecchina, A.; Bellussi, G. *J. Phys. Chem. B* **1997**, *101*, 4740.

(38) Frey, P. A.; Whitt, S. A.; Tobin, J. B. *Science* **1994**, *264*, 1927.

(39) Scott, A. P.; Radom, L. *J. Phys. Chem.* **1996**, *100*, 16502.

(40) Paukshtis, E. A.; Malysheva, L. V.; Stepanov, V. G. *React. Kinet. Catal. Lett.* **1998**, *65*, 145.

(41) Brändle, M.; Sauer, J. *J. Am. Chem. Soc.* **1998**, *120*, 1556.